# Protein–DNA Interactions and Alterations in the DNA Structure upon UvrB–DNA Preincision Complex Formation during Nucleotide Excision Repair in *Escherichia coli*†

R. Visse,* A. King, G. F. Moolenaar, N. Goosen, and P. van de Putte

*Leiden Institute of Chemistry, Laboratory of Molecular Genetics, Gorlaeus Laboratories, Leiden University, P.O. Box 9502, 2300 RA Leiden, The Netherlands*

*Received February 28, 1994; Revised Manuscript Received June 13, 1994*®

ABSTRACT: The UvrB–DNA preincision complex is a key intermediate in the repair of damaged DNA by the UvrABC endonuclease from *Escherichia coli*. DNaseI footprinting of this complex on DNA with a *cis*-[$Pt(NH_3)_2${d(GpG)-N7(1),N7(2)}] adduct provided global information on the protein binding site on this substrate [Visse, R., et al. (1991) *J. Biol. Chem. 266*, 7609–7617]. By applying a method developed by Fairall and Rhodes [Fairall, L., & Rhodes, D. (1992) *Nucleic Acids Res. 20*, 4727–4731], who have used the size and shape of DNaseI for the interpretation of a footprint, we were able to define in more detail the region where UvrB–DNA interactions in the preincision complex occur. The potential interactions with phosphate groups could be reduced to less then 14 in the damaged and to 12 in the nondamaged strand. The main UvrB–DNA interactions seem restricted to the major groove on both sides of the lesion. As a consequence UvrB crosses the minor groove just downstream of the damage. Such a binding of UvrB orients the protein away from the damage. The more detailed interpretation of UvrB–DNA interactions was supported by methylation protection experiments. The structure of the DNA in the preincision complex formed on *cis*-[$Pt(NH_3)_2${GpG-N7(1),N7(2)}] is altered as could be shown with diethylpyrocarbonate sensitivity of adenines just downstream of the lesion. However the adenines just downstream of another cisplatin adduct, *cis*-[$Pt(NH_3)_2${d(GpCpG)-N7(1),N7(3)}], did not become diethylpyrocarbonate sensitive in the preincision complex although this complex is incision proficient. Apparently this structural alteration is not a prerequisite for proficient preincision complex formation, UvrC binding, or incision. The UvrB–DNA preincision complex induced very mild $KMnO_4$ sensitivity of thymines in the nondamaged strand. In the presence of UvrA, UvrB, and UvrC however, there was a dramatic increase in the $KMnO_4$ sensitivity of thymines in the nondamaged strand near the 3′ incision position, which suggests that this region may become single stranded after incision. We propose that this single-stranded region near the 3′ incision site could be the entry site of UvrD for the release of the oligonucleotide containing the damage.

The UvrABC endonuclease from *Escherichia coli* is remarkably versatile in its capacity to repair structurally unrelated DNA lesions. The mechanism by which the three proteins UvrA, UvrB, and UvrC incise damaged DNA on both sides of a lesion has largely been resolved at a macromolecular level and has been the subject of a number of reviews (Grossman & Thiagalingam, 1993; Lin & Sancar, 1992a; Van Houten, 1990). In short, the recognition of a lesion in the DNA by the $UvrA_2B$ complex is followed by a conformational change in this nucleoprotein complex and results in the formation of the UvrB–DNA preincision complex (Orren & Sancar, 1989, 1990; Visse et al., 1992). Binding of UvrC to this complex induces UvrB to make the 3′ incision which is followed by the 5′ incision by UvrC (Lin et al., 1992; Lin & Sancar, 1992b). Subsequently the oligonucleotide containing the damage and UvrC are released by UvrD. The single-stranded gap is filled in by DNA polymerase I which releases UvrB (Orren et al., 1992). The repair is completed with the closure of the nick by DNA ligase. It is still not known, however, how the Uvr proteins interact with each other and with the damaged DNA and what the exact nature is of the conformational changes in the nucleoprotein complexes.

One of the more fundamental questions is how the $UvrA_2B$ complex is capable of recognizing the large variety of structurally unrelated DNA lesions. A comparison of the perturbation of the DNA by different lesions that are recognized by the UvrABC endonuclease did not reveal a structural feature shared by all substrates (Van Houten, 1990) although recently changes in base stacking interactions have been proposed as a common determinant in the recognition of damaged DNA (Van Houten & Snowden, 1993).

Another important aspect of the UvrABC endonuclease DNA excision repair reaction is that the positions of the incision sites seem to be largely independent of the type of damage. The DNA is incised on both sides of the lesion in general at comparable positions: the eighth phosphodiester bond 5′ and the fourth or fifth phoshodiester bond 3′ of the lesion. UvrC, which has no apparent affinity for UvrA or UvrB in solution (Orren & Sancar, 1989), binds to the preincision complex in which the DNA seems primed for incision. Apparently, for all the different lesions that are repaired, the preincision complexes share sufficient similarity to result in comparable incision sites.

The formation of a UvrB–DNA preincision complex is associated with significant changes in the DNA structure. These changes include about one helical turn unwinding (Oh & Grossman, 1986), formation of one or more DNaseI sensitive sites (Van Houten et al., 1987; Visse et al., 1991), the bending of the DNA observed with electron microscopy (Shi et al.,

† This work was supported by the J. A. Cohen Institute, Interuniversity Institute for Radiopathology and Radiation Protection (I.R.S.).

* Corresponding author.

® Abstract published in *Advance ACS Abstracts,* July 15, 1994.

0006-2960/94/0433-9881$04.50/0 

1992) and a decrease of the linear dichroism signal of the DNA (Takahashi et al., 1992). These changes are probably essential for the recognition and processing of the complex by UvrC. In this paper we have reexamined our previous DNaseI footprinting data of preincision complexes formed on DNA containing specific cisplatin adducts by taking into account the phosphate contacts and size of the DNaseI protein. Preincision complexes were further analyzed using different chemical footprinting methods. The combined footprinting results demonstrate that the major groove is bound by UvrB on both sides of the lesion and UvrB seems to cross the minor groove to connect these areas. The analysis of postincision complexes with $KMnO_4$ suggest that after incision significant structural changes occur which are most prominent near the 3′ incision site. On the basis of these findings, we propose a model for the mechanism of UvrD-induced release of the damage containing oligonucleotide.

## MATERIALS AND METHODS

*Protein Purification and DNA Substrates.* The UvrA, UvrB, and UvrC proteins were purified as described before (Visse et al., 1992). The construction of the synthetic 96 bp DNA fragments containing a site-specific *cis*-Pt·GG[1] or a *cis*-Pt·GCG adduct was as reported (Visse et al., 1991, 1994).

*Chemical Footprinting Methods.* DEPC footprinting was performed essentially according to Bateman and Paule (1988). UvrA and UvrB at the indicated concentrations were preincubated for 5 min at 37 °C in 20 μL containing 40 mM HEPES, pH 7.8, 10 mM $MgCl_2$, 1 mM ATP, 1 mM DTT, 0.1 mg/mL BSA, and 75 mM KCl. About 25 000 cpm (Cerenkov) of $^{32}$P-labeled DNA fragment was added together with 62.5 ng of pBR322 DNA, and the incubation was continued for 15 min. The incubation mixture was cooled to 25 °C and 1 μL of DEPC was added. The mixture was gently mixed every 5 min for a total incubation time of 15 min. The reaction was stopped by the addition of 80 μL of 10 mM imidazole and 0.5 μg of calf thymus DNA. The DNA was then isolated by phenol extraction and ethanol precipitation. Strand breaks were introduced by dissolving the DNA in 100 μL of 1 M piperidine and heating the sample for 30 min at 90 °C. The piperidine was removed by repeated coevaporation with water. Equal amounts of radioactivity were loaded on a 8% polyacrylamide 8 M urea gel. After the run the gel was dried on a filter and exposed to an X-Omat AR Kodak film.

$KMnO_4$ oxidation of thymines in perturbed B–DNA was essentially done as described by Jeppesen and Nielsen (1989). The reaction was performed in 20 μL of standard Uvr buffer, 50 mM Tris-HCl, pH 7.5, 10 mM $MgCl_2$, 1 mM ATP, 0.1 mg/mL BSA, and 75 mM KCl. DTT was omitted from the reaction mixture as this quenched the permanganate reaction. UvrA and UvrB were incubated at the indicated concentrations for 5 min at 37 °C, after which the $^{32}$P-labeled DNA fragment was added together with 62.5 ng of pBR322 DNA, 20 nM UvrC, and/or 5 or 20 nM UvrD where indicated. After incubation for another 20 min the reaction mixture was made 1 mM $KMnO_4$, and after 1 min the oxidation was stopped with 10 μL of 1.5 M NaAc, 1 M 2-mercapthoethanol, and 200 ng of calf thymus DNA. The DNA was recovered with ethanol precipitation, and, after a piperidine treatment as described above, the DNA was analyzed on a 8% polyacrylamide 8 M urea gel.

For the methylation protection experiments UvrA and UvrB were preincubated at 37 °C for 5 min in standard Uvr buffer. After the addition of the $^{32}$P-labeled DNA fragments and an additional 15-min incubation, 1 μL of a fresh 1:250 dilution of DMS in water was added. After 5 min the methylation reaction was stopped by addition of 20 μL of 1 M 2-mercapthoethanol and 50 ng/μL calf thymus DNA. The DNA was recovered by ethanol precipitation, piperidine treated, and run on a gel as described above.

## RESULTS

*DNase I and MPE Footprints.* We have applied the DNaseI footprinting method on the UvrB–DNA preincision complex formed with synthetic DNA containing a single *cis*-Pt·GG adduct (Figure 1; Visse et al., 1991, 1992). In this complex an area of approximately 20 bp is protected against DNaseI degradation (Figure 1A), which is comparable to the results obtained by others using different damaged-DNA substrates (Seeberg & Fuchs, 1990; Van Houten et al., 1987). The resolution of the DNaseI footprint technique, however, is limited, giving only a global impression of the area of protein binding. Recently Fairall and Rhodes (1992) very elegantly used the information derived from DNaseI–DNA cocrystals (Lahm & Suck, 1991; Suck et al., 1988) to get more detailed information on the binding of TFIIIA from a footprint of the TFIIIA–5S DNA complex. DNaseI is known to bind to the minor groove, and its activity is dependent on the minor groove width and the bendability of the DNA [for a review, see Travers (1989)]. The protein contacts two phosphates on either side of the incision position and two phosphates across the minor groove. The binding of DNaseI covers the minor groove and the major groove adjacent to the cleavage site (Figure 1A). The size and shape of DNaseI can be used to delimit the space that is occupied by the protein of interest.

Using this approach, we have reexamined our previously determined DNaseI footprints of the UvrB–DNA preincision complex on DNA containing a *cis*-Pt·GG adduct (Visse et al., 1991, 1992). The results are summarized in a schematic two-dimensional presentation of a DNA double helix (Figure 1A). The phosphates that are available for the contacts with DNaseI cannot be involved in UvrB–DNA interactions. This means that in the damaged strand only 14 and in the nondamaged strand only 12 potential sites remain for UvrB–phosphate interactions (Figure 1B). Figure 1A shows that large parts of the minor groove of the DNA within the DNaseI footprint are not involved in UvrB-binding. The major groove areas that remain for UvrB-binding are on both sides of the platinum adduct.

To further reduce the area accessible to UvrB, we also included in Figure 1A the areas in the preincision complex that display enhanced sensitivity toward the intercalating footprinting agent MPE (Visse et al., 1991). MPE intercalates in the DNA via the minor groove where hydroxyl radicals are generated. These diffusible radicals attack the 1′ or 4′ position of the deoxyribose moiety (Dervan, 1986; Hertzberg & Dervan, 1984). In the patches of enhanced sensitivity in the preincision complex that span the minor groove from 43–46 and from 55–60 (Figure 1A), the DNA must be accessible to MPE and the sugar positions to the hydroxyl radicals. As a consequence UvrB cannot be bound to this part of the minor groove.

The combined results indicate that the area that is accessible to UvrB–DNA contacts in the preincision complex is limited to the minor groove from position 46–54 and 45′–51′ in the

[1] Abbreviations: *cis*-Pt·GG, *cis*-[Pt(NH$_3$)$_2${d(GpG)-N7(1),N7(2)}]; *cis*-Pt·GCG, *cis*-[Pt(NH$_3$)$_2${d(GpCpG)-N7(1),N7(3)}]; cisplatin, *cis*-diamminedichloroplatinum(II); DEPC, diethylpyrocarbonate; DMS, dimethyl sulfate; $KMnO_4$, potassium permanganate; MPE, methidium-propyl-EDTA; $OsO_4$, osmium tetraoxide.

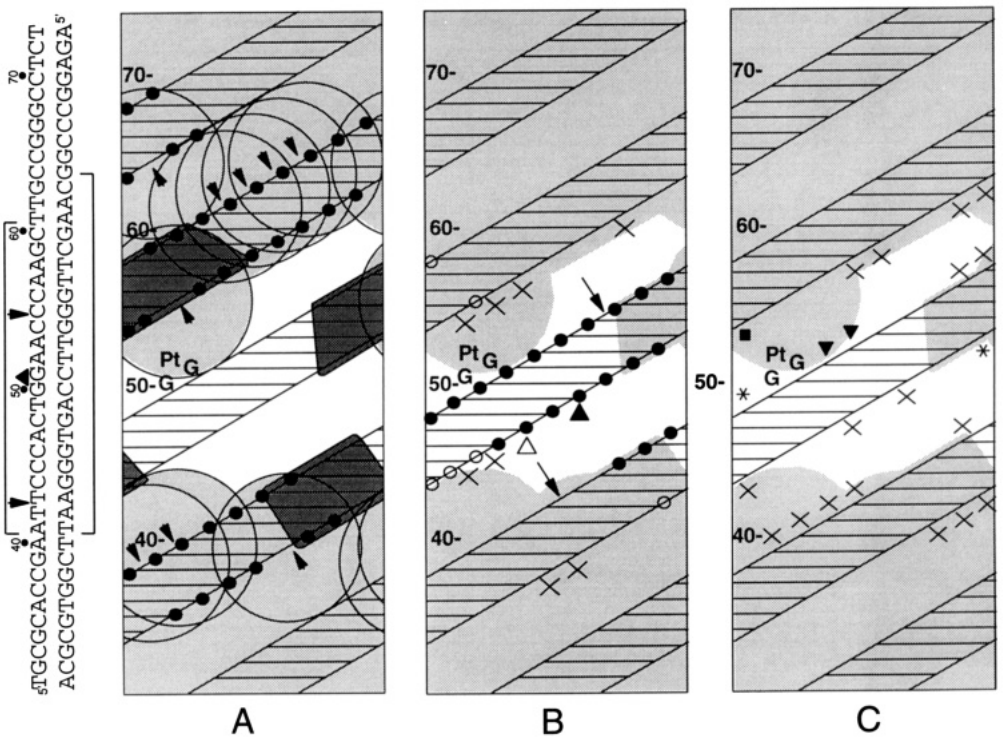


FIGURE 1: Schematic summary of the results. (A) Schematic representation of the DNaseI cleavage sites, DNaseI phosphate contacts, and the space occupied by DNAseI in a footprint of the UvrB–DNA preincision complex. The data are presented in a two-dimensional cylindrical projection of a DNA double helix. The base pairs are indicated as horizontal lines across the minor groove. The strand containing the *cis*-Pt·GG at positions 50 and 51 is numbered (N). The numbering of the nondamaged strand (N′) corresponds to that of the damaged strand. The corresponding sequence is given on the left, and the area of DNA that is protected against DNaseI cleavage in the preincision complex and the position of UvrC-induced incision are indicated (Visse et al., 1991, 1992). The DNaseI molecules are shown as overlapping circles, each making two phosphate contacts (closed circles) on both sides of the incision position (arrow) and two more phosphate contacts across the minor groove. Only those DNaseI molecules are shown that define the border of potential UvrB–DNA interactions. The remainder of the DNA which is also accessible to DNaseI is shaded only for clarity. A single site at position 56′ in the undamaged bottom strand that remains sensitive to DNaseI degradation in the UvrB–DNA complex is shown as well. The areas of enhanced MPE sensitivity (Visse et al., 1991) are darkly shaded. The unshaded area remains for potential UvrB–DNA interactions. (B) Summary of the methylation protection footprinting. The shaded area is accessible to either DNaseI or MPE, the unshaded area remains for potential UvrB–DNA interactions (see panel A). Guanine 48′ (closed triangle) is protected against methylation in the preincision complex, whereas guanine 46′ (open triangle) becomes hypersensitive to methylation. The methylation of the guanines that remain unaffected by the preincision complex formation are indicated by an X. Also indicated in this scheme are the positions of the phosphates that do not interact with DNaseI (open and closed circles; compare panel A). Those phosphates that on the basis of their position seem to have a low probability to interact with UvrB are indicated as open circles. The positions of 5′ and 3′ incisions that were determined before (Visse et al., 1991) are shown as arrows. (C) Summary of the $KMnO_4$ and DEPC footprinting of the preincision complex on *cis*-Pt·GG containing DNA. The potential UvrB–DNA contacts are limited to the unshaded area (see panel A). Cisplatin-induced sensitivity of thymines 49 and 52′ is shown by an asterisk. The preincision complex induced mild sensitivity of thymine 53′ is represented by a closed square. The adenines 52 and 53 that become hypersensitive to DEPC in the preincision are indicated with a closed triangle. Adenines or thymines that do not show increased reactivity towards either $KMnO_4$ or DEPC are marked with an X.

damaged and nondamaged strand, respectively. The major groove areas available for UvrB-binding are situated on both sides of the lesion, from position 42–48 and 53–57 relative to the damaged strand. This places UvrB on the opposite site of the DNA helix as the cisplatin adduct.

*Methylation Protection.* In order to obtain more detailed information on UvrB–DNA contacts, we performed guanine methylation protection footprinting. The interaction of UvrB with the DNA is mainly a hydrophobic one, possibly by intercalation of amino acid residues between the base moieties (Van Houten & Snowden, 1993). As discussed above, the main interactions of UvrB with the DNA are in the major groove and one could therefore expect that these interactions may interfere with the methylation of the guanine N7 which is situated in the major groove. We could investigate methylation protection in the undamaged strand only since the damaged strand does not contain guanines in the area of UvrB binding other than those platinated which consequently are not sensitive to methylation. No alterations in the methylation pattern were seen with UvrA alone (results not shown). Results show that the methylation of two guanines is altered by the presence of a preincision complex on the DNA (Figure 2 and schematically in Figure 1B). Guanine 48′ is protected against methylation and must therefore be in close contact with UvrB in the preincision complex. Guanine 48′ is located in the middle of the major groove area bound by UvrB (Figure 1B) which explains its protection. Guanine 46′, on the other hand, becomes hypersensitive to methylation. Since guanine 46′ is on the border of the proposed region where UvrB contacts the DNA, this hypersensitivity could be the result of a hydrophobic pocket formed at this border thereby locally increasing the concentration of DMS which is sparsely soluble in water (Nielsen, 1990). No change in methylation pattern was observed for guanines at positions 37′, 38′, 44′, 45′, 54′, 55′, 56′, and 60′. This is in agreement with the area of UvrB–DNA interactions based on the DNaseI and MPE footprints presented above since these bases are positioned on the border of or outside the area of UvrB–DNA interactions (Figure 1B).

*Footprinting with Structure Sensitive Probes $KMnO_4$ and DEPC.* The formation of the UvrB–DNA preincision complex results in structural changes of the DNA. These changes are not always the same since we have observed differences in the number of DNaseI sensitive sites on preincision complexes formed with *cis*-Pt·GG or *cis*-Pt·GCG containing DNA (Visse et al., 1994). For more details we probed the preincision

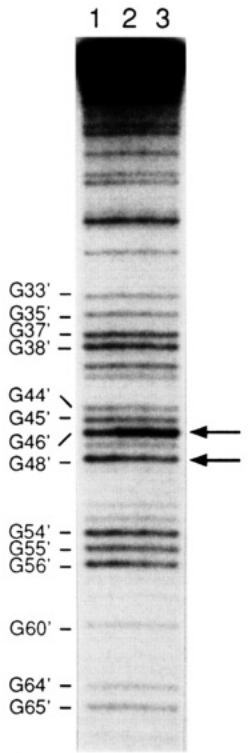


FIGURE 2: Methylation protection by UvrB in the UvrB–DNA preincision complex. The *cis*-Pt·GG containing 96 bp fragment was labeled 5′ in the bottom strand and incubated with UvrB alone (100 nM) or with 5 or 25 nM UvrA together with 100 nM UvrB, lanes 1–3, respectively. After a 15-min incubation at 37 °C, 1 μL of a fresh 1:250 DMS dilution was added, and the incubation continued for 5 min. The reaction was stopped and the DNA analyzed as described under Materials and Methods. The positions of the relevant guanines are indicated. The results are summarized in Figure 1B.

complexes on both lesions with $KMnO_4$ and DEPC, chemicals that respond to the conformation of the DNA.

$KMnO_4$ can oxidize the 5,6 double bond of thymines, forming a thymine diol. In B-DNA, however, the 5,6 double bond of thymine is shielded by stacking interactions of the bases. Therefore perturbation of this stacking will increase the sensitivity of thymine for oxidation. $KMnO_4$ has been successfully used to show the unpaired thymines in the RNA polymerase–promoter open complex (Jeppesen & Nielsen, 1989; Sassa-Dwight & Gralla, 1989) and also to demonstrate more subtle deformations in the DNA caused by intercalating agents (Fox & Grigg, 1988; Jeppesen & Nielsen, 1988). The minimal distortion needed to increase thymine sensitivity is not known but unwinding which would involve changes in base pair distances, tilt, and twist angles are expected to influence the thymine oxidation (Nielsen, 1990).

First we examined the effect of the cisplatin lesion itself on the sensitivity of the DNA towards $KMnO_4$. In the *cis*-Pt·GG fragment, thymine 49 in the damaged strand was found to be sensitive to oxidation due to the platinum adduct (Figure 3A and Figure 1C). Such a sensitivity cannot be detected in the case of the *cis*-Pt·GCG containing DNA since this fragment has a cytosine at this position ($CCG_{50}CGAACC$ versus $CTG_{50}GAACCC$). In the bottom strand *cis*-Pt·GG induces mild $KMnO_4$ sensitivity of the thymine at position 52′ (Figure 3B). This position is not very sensitive to oxidation in the *cis*-Pt·GCG containing DNA.

When we probed the DNA fragments in the presence of UvrA or UvrA and UvrB, no additional $KMnO_4$ sensitive thymines in the damaged strand were found for both the *cis*-Pt·GG and *cis*-Pt·GCG DNA fragments (Figure 3A). Also

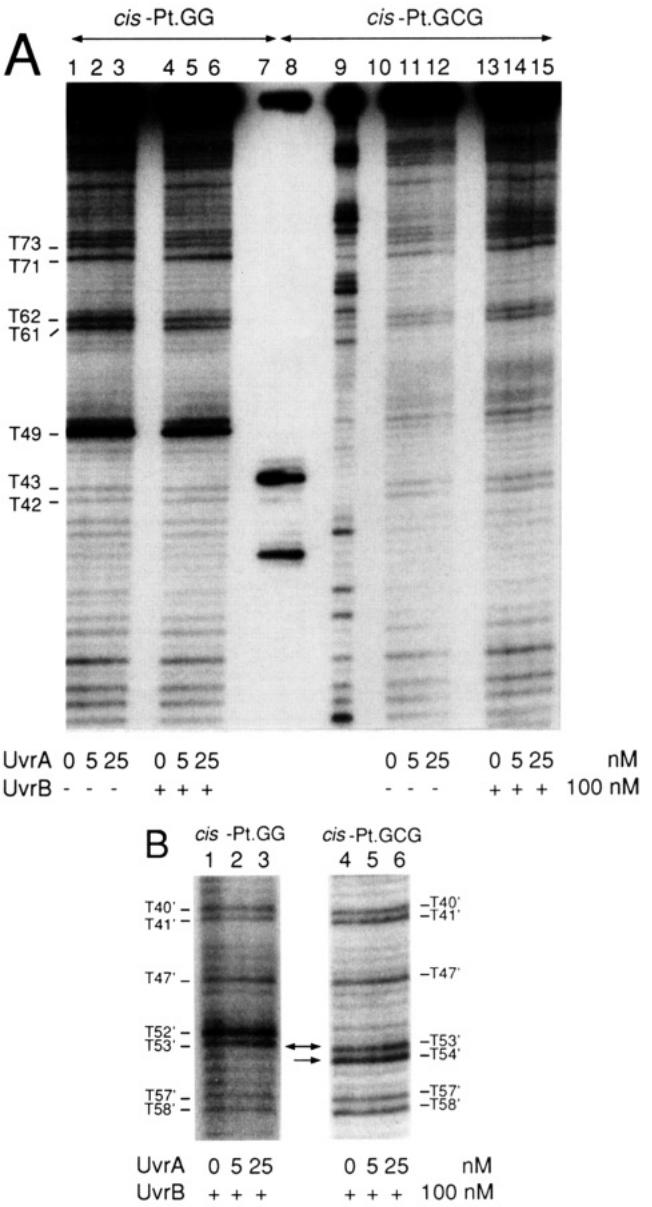


FIGURE 3: $KMnO_4$ probing of preincision complexes on *cis*-Pt·GG and *cis*-Pt·GCG DNA. (A) The DNA was 5′ $^{32}$P-labeled in the damaged strand. (Lanes 1–7) DNA fragment containing *cis*-Pt·GG; (lanes 8–15) *cis*-Pt·GCG containing DNA. The DNA in lanes 1–6 and 10–15 was incubated with indicated amounts of UvrA and UvrB under conditions described under Materials and Methods. (Lanes 7 and 8) Incision of the DNA *cis*-Pt·GG and *cis*-Pt·GCG fragments, respectively, by UvrABC under the same conditions, but without the $KMnO_4$ incubation. Lane 9 is a G-lane. ( B) *cis*-Pt·GG (lanes 1–3) or *cis*-Pt·GCG (lanes 4–6) containing fragments 5′ $^{32}$P-labeled in the nondamaged strand were incubated with UvrA and UvrB as indicated and probed with $KMnO_4$ as described. Arrows indicate the thymines that become slightly more sensitive to oxidation as a result of preincision complex formation.

with UvrA alone no changes in $KMnO_4$ sensitivity were found in the nondamaged strand (results not shown). Only some minor effects of the preincision complex on the $KMnO_4$ sensitivity of the thymines in the nondamaged strand were observed. For the *cis*-Pt·GG fragment thymine 53′ became slightly sensitive to oxidation (Figure 3B and schematically in Figure 1C). The preincision complex on the *cis*-Pt·GCG slightly sensitized thymines 53′ and 54′ (Figure 3B). No alterations in the sensitivity of thymines 40′, 41′, 47′, 57′, and 58′ were seen in either substrate. This suggests that in the UvrB–DNA complex the distortion of these thymines in both substrates is very minor or that they are shielded by UvrB.

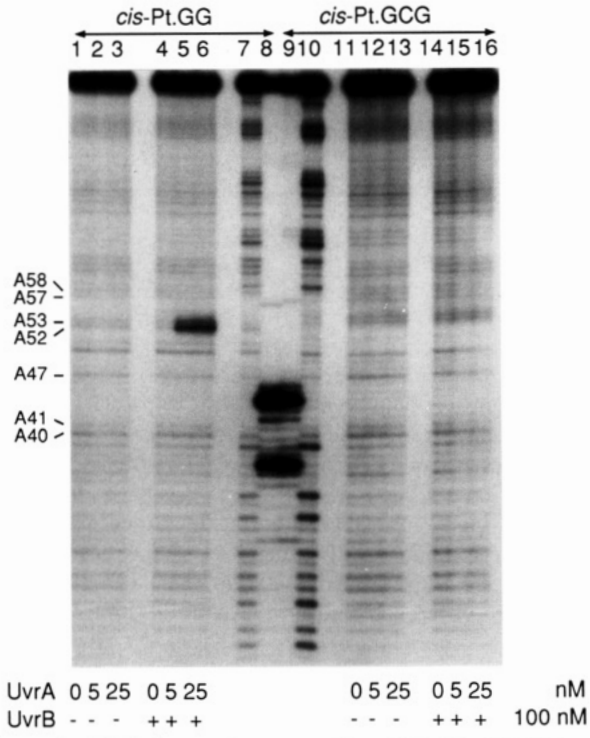


FIGURE 4: Diethylpyrocarbonate probing of the UvrB–DNA preincision complexes. The DNA fragments containing a *cis*-Pt·GG (lanes 1–8) or a *cis*-Pt·GCG adduct (lanes 9–16) and 5′ $^{32}$P-labeled in the damaged strand were incubated with UvrA and UvrB as shown (lanes 1–6 and 11–16). DEPC treatment was as described under Materials and Methods. In lanes 8 and 9, the *cis*-Pt·GG and *cis*-Pt·GCG containing DNA was treated with UvrABC under the same conditions but without the DEPC treatment. Lanes 7 and 10 are G-lanes of the *cis*-Pt·GG and *cis*-Pt·GCG containing DNA fragments, respectively.

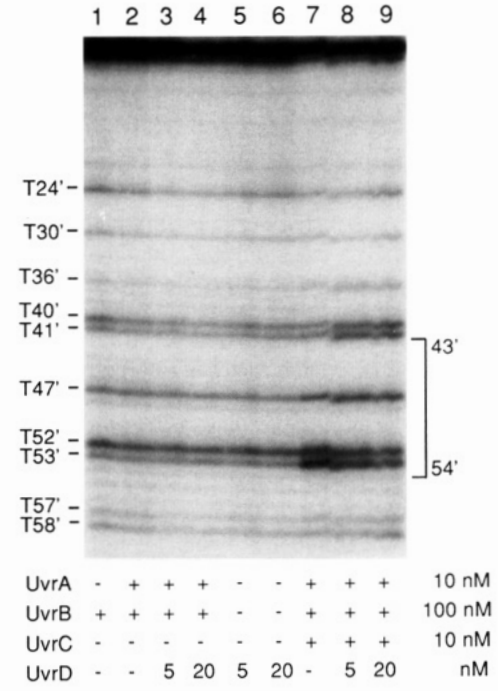


FIGURE 5: Effect of incision and postincision events on $KMnO_4$ sensitivity. The *cis*-Pt·GG containing DNA fragment was labeled 5′ in the nondamaged strand, incubated with various combinations of Uvr subunits as indicated, and subsequently treated with $KMnO_4$ as described under Materials and Methods. The positions of the thymines in the nondamaged strand and the size of the single-stranded gap that results from the release of the damaged oligo from the complementary strand are indicated.

DEPC is a purine specific reagent which carbetoxylates the N7 position leading to ring opening of the purine moiety. The subsequent hydrolysis of the glycosidic bond then results in strand scission under alkaline conditions (Vincze et al., 1973). Probably because of the size of DEPC, the N7 of purines in the major groove is not accessible in B-DNA. However, when the N7 position of purines is more exposed as in Z-DNA or in ss-DNA the reactivity toward DEPC is strongly increased (Herr, 1985; Johnston & Rich, 1985). The minimal deformation of B-DNA needed to increase the DEPC reactivity toward the purines is not known, but based on the work on bis-intercalating agents unwinding of the helix without disrupting base-pairing may be sufficient (Jeppesen & Nielsen, 1988; McLean & Waring, 1988).

Unlike $KMnO_4$ the presence of the *cis*-Pt·GG or *cis*-Pt·GCG itself did not result in DEPC sensitivity (Figure 4, lanes 1 and 11). However, under conditions that allow preincision complex formation two strong DEPC sensitive sites are observed with *cis*-Pt·GG (Figure 4, lanes 5 and 6). Sensitivity for DEPC was not observed on nondamaged DNA (not shown) or in the presence of only UvrA (lanes 2 and 3) or only UvrB (lane 4). The preincision complex dependent DEPC hypersensitive sites correspond to adenines 52 and 53 in the top strand. These adenines are positioned directly 3′ of the *cis*-Pt·GG adduct (Figure 1C). Although in the autoradiogram of Figure 4 the band corresponding to position adenine 52 is more intense than for adenine 53, we found that both positions are equally sensitive to DEPC because in a 3′-labeled fragment the intensities of the bands were found to be reversed (not shown). No DEPC sensitivity was observed with the adenines 40, 41, 47, 57, and 58. Also no DEPC sensitivity of the adenines in the nondamaged strand at positions 42′, 43′, and 49′ was seen (results not shown; schematically in Figure 1C). This indicates either that these positions are not perturbed by the preincision complex or that they are protected by UvrB. In none of our experiments did we observe DEPC sensitivity of guanines, which could be due to the fact that they are less reactive than adenines.

Surprisingly, the *cis*-Pt·GCG containing DNA fragment (Figure 4, lanes 8–16) did not show any DEPC hypersensitivity in the damaged strand under conditions that allow UvrB–DNA preincision complex formation, although also in this construct two adenines are present directly downstream of the adduct (lanes 15 and 16; $CCG_{50}CGAACC$). Also no preincision complex induced sensitivity was observed in the nondamaged strand (results not shown).

To demonstrate that preincision complexes are proficiently formed on both *cis*-Pt·GG and *cis*-Pt·GCG containing DNA, the fragments were incubated with UvrA, UvrB, and UvrC in the same buffer as used for the DEPC treatment. Incisions were observed at the 8th and the 15th phosphodiester bond upstream of the lesion for both fragments as described before (Figure 4, lanes 8 and 9; Visse et al., 1991, 1992). This shows that the lack of DEPC sensitivity of the *cis*-Pt·GCG–preincision complex is due to a different local DNA conformation of this complex and not to the inability to form a preincision complex.

*Effects of Incision and Postincision Events on the DNA Structure.* Incubation of a damaged DNA fragment with UvrA, UvrB, and UvrC results in incision of the DNA on both sides of the lesion. The *cis*-Pt·GG containing DNA fragment, 5′ labeled in the nondamaged strand, was probed with $KMnO_4$ under these conditions to determine the effect of incision on the DNA structure (Figure 5). The results show a dramatic increase in the sensitivities of thymines 52′ and 53′ toward oxidation. Thymine 47′ became moderately

sensitive whereas no effect was seen for the thymines at positions 40′ and 41′, which are positioned close to the 5′ incision site. The results indicate a significant conformational change in the DNA as a result of the incision which is most prominent near the 3′ incision site. This conformational change is possibly the result of DNA unwinding or even unpairing of the bases.

When UvrD was included in the incubation mixture with UvrA, UvrB, and UvrC, thymines 40′ and 41′ also became more sensitive to oxidation (Figure 5, compare lane 7 with 8 and 9). This sensitivity is probably the result of the release of the damaged oligonucleotide. The sensitivity of thymines 52′ and 53′ is not further increased suggesting that these were already unpaired in the presence of UvrABC (Figure 5, lane 7). None of the thymines at positions 36′, 57′, and 58′ displayed any increased sensitivity. Therefore sensitivity in the nondamaged strand is restricted to thymines in or at the border of the single-stranded region (positions 42′–54′/55′) that is the result of the release of the oligonucleotide.

## DISCUSSION

Reinterpretation of our DNaseI and MPE footprint data enabled us to more precisely define the area of potential UvrB–DNA interactions in the preincision complex (Figure 1A). This area is limited to the minor groove positions 46–54 in the damaged strand and positions 45′–51′ in the nondamaged strand, respectively. The major groove areas available for UvrB are found on both sides of the lesion, positions 42–48 and 53–57 with respect to the damaged strand. These major groove areas can only be connected by one UvrB molecule when the protein crosses the minor groove just downstream of the lesion. Evidence for major groove contacts upstream of the lesion was obtained with methylation protection footprinting (Figure 1B). The potential phosphate contacts that UvrB can make were reduced to 14 and 12 in the damaged and nondamaged strand, respectively (Figure 1B). Given their position relative to the binding of UvrB, six of these remaining phosphates seem unlikely to be involved in UvrB–DNA contacts (open circles in Figure 1B). This would leave 13 phosphate groups (positions 45–57) in the damaged and seven (positions 46′–52′) in the nondamaged strand. Experiments to determine the phosphate contacts of UvrB directly with ethylnitrosurea have been unsuccessful thus far.

In our model it seems that the two major groove areas where UvrB is bound are mainly located on the opposite site of the helix relative to the damage (Figure 1). This is supported by the observation that a thymine dimer in a preincision complex is still accessible for photolyase (Sancar et al., 1984). Such an orientation of UvrB with respect to the damage would lower the probability that bulky adducts interfere directly with the formation of the preincision complex and is likely to contribute to the proficiency of the UvrABC endonuclease to process totally different lesions. In the model, UvrB is crossing the minor groove just downstream of the lesion. This results in a close contact with the 3′ incision site which agrees with the observation that the 3′ incision is made by UvrB (Lin et al., 1992). The 5′ incision is made by UvrC (Lin & Sancar, 1992b) and, indeed, the phosphates around this site are not bound by UvrB (Figure 1B).

Our model also may help to explain the results obtained by Svoboda et al. (1993). They showed that incision of DNA containing a thymine dimer in one strand with an additional dimer in the complementary strand depends on the relative position of these dimers. The DNA is incised when the two dimers are 5′ staggered, but the DNA is refractory to incision when the orientation is 3′ staggered. Projected in our schematical helix (Figure 1) and assuming the first dimer at positions 50 and 51, the position of a 5′ staggered dimer would be at positions 52′–53′, which is at the border of the area of UvrB-binding and could explain why it does not interfere with preincision complex formation. A 3′ staggered dimer on the other hand would coincide with positions 48′–49′, which is in the middle of the major groove area where UvrB is bound. Therefore 3′ staggered dimers, and in fact any 3′ staggered lesions, are likely to interfere with UvrB–DNA preincision complex formation.

The perturbation of the DNA by the *cis*-Pt·GG adduct could be shown by the increased sensitivity of two thymines toward oxidation. The thymine located just upstream of the lesion in the damaged strand is more sensitive than the thymine directly downstream in the nondamaged strand. Schwartz et al. (1989) have probed the *cis*-Pt·GG adduct on a double-stranded 8-mer (dTCTGGTCT; residues identical to our fragment are underlined) using $OsO_4$ but observed no sensitivity of any of the thymines near the platinum adduct. Although the difference could be due to the difference in length of the DNA fragments, it is more likely the result of the oxidizing agent used. Like $KMnO_4$, $OsO_4$ also oxidises the 5,6 double bond of thymine, but the molecule is larger and has less oxidizing power. Apparently, $KMnO_4$ is a more sensitive probe for the detection of structural changes in the DNA.

All the distortions of the DNA in the preincision complex that could be measured with $KMnO_4$ and DEPC are situated close to the lesion (Figure 1C). This could mean that preincision complex induced alteration of the DNA structure is confined to the site of the lesion. However, it has been postulated that the preincision complex formation is accompanied with one helical turn unwinding (Oh & Grossman, 1986) suggesting that the conformational changes should be more than we observe in our experiments. The unwinding of the DNA could be through intercalation of hydrophobic amino acid side chains of UvrB in the DNA (Van Houten & Snowden, 1993). In view of our model this unwinding is expected to occur from the major groove side. Therefore it is very likely that in the preincision complex UvrB shields the reactive sites of the perturbed bases in the major groove. The observed patches of enhanced MPE intercalation in the minor groove (Figure 1A) could be a consequence of the UvrB mediated DNA unwinding.

The DEPC sensitive sites observed just downstream of the *cis*-Pt·GG lesion are absent in the preincision complex formed with *cis*-Pt·GCG, indicating that the structure of the DNA in the preincision complex in the direct vicinity of the lesion is different in both cases. We have shown before, however (Visse et al., 1994), that the preincision complex formation and subsequent UvrC binding on *cis*-Pt·GG and *cis*-Pt·GCG containing DNA are of comparable efficiencies. Apparently the structure that is detected by the DEPC sensitivity is not a prerequisite for the formation of an incision proficient preincision complex. As UvrB makes most contacts with the DNA flanking the lesion, the structure of the DNA around the lesion is the net effect of the structure imposed by UvrB and the structure of the lesion in the first place. For some lesions the consequence could be localized unwinding at the site of the lesion with unpairing as an extreme form and for other lesions the local structure may be hardly affected. That different structures of the DNA near the lesion are allowed in the preincision complex might also contribute to the ability

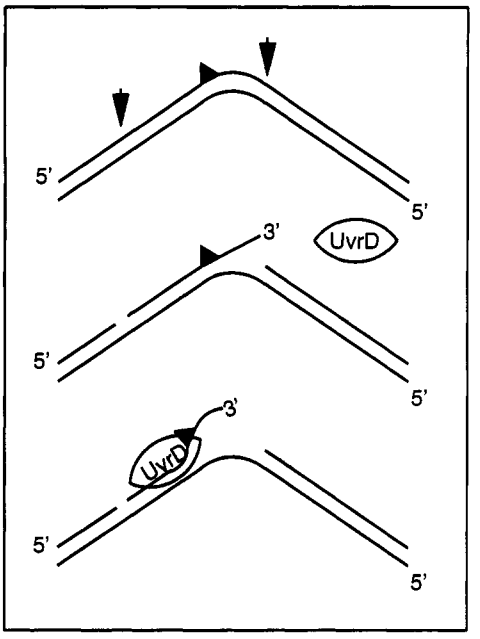


FIGURE 6: Unpairing of the 3′ end of the damaged oligo may serve as an entry site for UvrD. The DNA in the preincision complex is bent, which may put a considerable stress on the DNA. Upon incision, the unpairing of the 3′ end of the damaged oligonucleotide may release this tension. This free 3′ end of the damaged oligonucleotide could then serve as an entry site for UvrD to release this oligonucleotide and UvrC.

of the UvrABC endonuclease to process such a variety of substrates.

As a result of the preincision complex formation, very mild $KMnO_4$ sensitive sites were induced. The addition of UvrC, however, resulted in a dramatic increase of the sensitivity of thymines in the nondamaged strand near the 3′ incision site, indicating a drastic change in the DNA structure near this site. In view of the strength of the signal, these thymines may be unpaired. This could mean that the complementary 3′ end of the damaged oligonucleotide is no longer base-paired. Such an unpairing could be a way to release tension in the DNA after incision (Figure 6). When UvrD was added to the reaction mixture, in addition thymines in the nondamaged strand close to the 5′ incision site became moderately sensitive, most likely a reflection of the release of the damaged oligonucleotide. That not all thymines in the single-stranded region become equally sensitive may be because UvrB remains bound (Orren et al., 1992). UvrD is a helicase with a 3′ → 5′ polarity (Matson, 1986). It has a preference to unwind DNA with a single-stranded region but, at higher concentrations, is capable of DNA unwinding from a nick or a blunt end (Matson, 1986; Runyon et al., 1990; Runyon & Lohman, 1989). There is no experimental evidence where UvrD binds in the postincision complex, but it is generally assumed that it binds to the nondamaged strand opposite the 5′ nick moving along the DNA in the same direction as DNA polymerase I as proposed by Matson (1986). A consequence of such a model is that UvrD has to bind to the same strand to which UvrB is already bound, and it has been shown that the UvrB protein is not released by the action of UvrD (Orren et al., 1992). The results presented in this paper suggest that a 3′ single-stranded region on the damaged oligonucleotide might be available as an entry site for UvrD. This could mean that UvrD binds to the displaced strand. That UvrD is able to bind to the displaced strand is supported by its activities in mismatch repair [for a review, see Modrich (1991)]. Recently, it was shown that the repair of a mismatch can be initiated from a hemimethylated d(GATC) site either 5′ or 3′ relative to the mismatch (Cooper et al., 1993; Grilley et al., 1993). This indicates that the nick in the DNA at the d(GATC) site does not determine the directionality of UvrD and that UvrD can unwind the DNA either bound to the displaced strand or to the nondisplaced strand. A consequence of binding to the displaced strand in the postincision complex is that the release of only the damaged oligonucleotide is ensured, which is reflected in the observation of a repair patch that coincides with the released oligo (Sibghat-Ullah et al., 1990).

## ACKNOWLEDGMENT

Dr. P. Emmerson is kindly acknowledged for his gift of UvrD. We are indebted to N. Boogaard for critical reading of the manuscript and modeling part of the 96 bp fragment which greatly facilitated interpreting our footprinting results.

## REFERENCES

Bateman, E., & Paule, M. R. (1988) *Mol. Cell. Biol. 8*, 1940–1946.
Cooper, D. L., Lahue, R. S., & Modrich, P. (1993) *J. Biol. Chem. 268*, 11823–11829.
Dervan, P. B. (1986) *Science 232*, 464–471.
Fairall, L., & Rhodes, D. (1992) *Nucleic Acids Res. 20*, 4727–4731.
Fox, K. R., & Grigg, G. W. (1988) *Nucleic Acids. Res. 16*, 2063–2075.
Grilley, M., Griffith, J., & Modrich, P. (1993) *J. Biol. Chem. 268*, 11830–11837.
Grossman, L., & Thiagalingam, S. (1993) *J. Biol. Chem. 268*, 16871–16874.
Herr, W. (1985) *Proc. Natl. Acad. Sci. U.S.A. 82*, 8009–8013.
Hertzberg, R. P., & Dervan, P. B. (1984) *Biochemistry 23*, 3934–3935.
Jeppesen, C., & Nielsen, P. E. (1988) *FEBS Lett. 231*, 172–176.
Jeppesen, C., & Nielsen, P. E. (1989) *Nucleic Acids Res. 17*, 4947–4956.
Johnston, B. H., & Rich, A. (1985) *Cell 42*, 713–724.
Lahm, A., & Suck, D. (1991) *J. Mol. Biol. 222*, 645–667.
Lin, J. J., & Sancar, A. (1992a) *Mol. Microbiol. 6*, 2219–2224.
Lin, J. J., & Sancar, A. (1992b) *J. Biol. Chem. 267*, 17688–17692.
Lin, J. J., Phillips, A. M., Hearst, J. E., & Sancar, A. (1992) *J. Biol. Chem. 267*, 17693–17700.
Matson, S. W. (1986) *J. Biol. Chem. 261*, 10169–10175.
McLean, M. J., & Waring, M. J. (1988) *J. Mol. Recognit. 1*, 138–151.
Modrich, P. (1991) *Annu. Rev. Genet. 25*, 229–253.
Nielsen, P. E. (1990) *J. Mol. Recognit. 3*, 1–25.
Oh, E. Y., & Grossman, L. (1986) *Nucleic Acids Res. 14*, 8557–8570.
Orren, D. K., & Sancar, A. (1989) *Proc. Natl. Acad. Sci. U.S.A. 86*, 5237–5241.
Orren, D. K., & Sancar, A. (1990) *J. Biol. Chem. 265*, 15796–15803.
Orren, D. K., Selby, C. P., Hearst, J. E., & Sancar, A. (1992) *J. Biol. Chem. 267*, 780–788.
Runyon, G. T., & Lohman, T. M. (1989) *J. Biol. Chem. 264*, 17502–17512.
Runyon, G. T., Bear, D. G., & Lohman, T. M. (1990) *Proc. Natl. Acad. Sci. U.S.A. 87*, 6383–6387.
Sancar, A., Franklin, K. A., & Sancar, G. B. (1984) *Proc. Natl. Acad. Sci. U.S.A. 81*, 7397–7401.
Sassa-Dwight, S., & Gralla, J. D. (1989) *J. Biol. Chem. 264*, 8074–8081.
Schwartz, A., Marrot, L., & Leng, M. (1989) *Biochemistry 28*, 7975–7989.
Seeberg, E., & Fuchs, R. P. P. (1990) *Proc. Natl. Acad. Sci. U.S.A. 87*, 191–194.

Shi, Q., Thresher, R., Sancar, A., & Griffith, J. (1992) *J. Mol. Biol. 226*, 425–432.
Sibghat-Ullah, Sancar, A., & Hearst, J. E. (1990) *Nucleic Acids Res. 18*, 5051–5053.
Suck, D., Lahm, A., & Oefner, C. (1988) *Nature 332*, 464–468.
Svoboda, D. L., Smith, C. A., Taylor, J. S., & Sancar, A. (1993) *J. Biol. Chem. 268*, 10694–10700.
Takahashi, M., Bertrand-Burggraf, E., Fuchs, R. P. P., & Nordén, B. (1992) *FEBS 314*, 10–12.
Travers, A. A. (1989) *Annu. Rev. Biochem. 58*, 427–452.
Van Houten, B. (1990) *Microbiol. Rev. 54*, 18–51.
Van Houten, B., & Snowden, A. (1993) *BioEssays 15*, 51–59.
Van Houten, B., Camper, H., Sancar, A., & Hearst, J. E. (1987) *J. Biol. Chem. 262*, 13180–13187.
Vincze, A., Hinderson, R. E. L., McDonald, F. F., & Leonard, N. J. (1973) *J. Am. Chem. Soc. 95*, 2677–2682.
Visse, R., de Ruijter, M., Brouwer, J., Brandsma, J. A., & van de Putte, P. (1991) *J. Biol. Chem. 266*, 7609–7617.
Visse, R., de Ruijter, M., Moolenaar, G. F., & van de Putte, P. (1992) *J. Biol. Chem. 267*, 6736–6742.
Visse, R., van Gool, A. J., Moolenaar, G. F., de Ruijter, M., & van de Putte, P. (1994) *Biochemistry 33*, 1804–1811.